Supplementary Materials for "A hybrid model for river water temperature as a function of air temperature and discharge"

Marco Toffolon and Sebastiano Piccolroaz
Department of Civil, Environmental and Mechanical Engineering,
University of Trento, Italy.

October 4, 2015

Corresponding author: Marco Toffolon, Department of Civil, Environmental and Mechanical Engineering, University of Trento, Italy. (marco.toffolon@unitn.it)

1 Introduction

These Supplementary Materials contain further details on the three case studies, the derivation of the main equation of the *air2water* model, the derivation of some analytical solutions, and the description of the Particle Swarm Optimization algorithm. The results obtained with the other versions of *air2water* different from the original 8-parameter formulation are shown in Figure 2, and the values of the model parameters are reported in Table 1. Moreover, Figure 3 shows the performance of the equilibrium approximation for the 8-parameter model. Finally, the performances of the logistic function model, one of the most popular nonlinear regression model, are reported in Figure 5 and Table 3.

2 Case Studies

The location of the three rivers used as cases studies is shown in Figure 1. Further details are listed below.

1. River Mentue at Yvonand (MAH-2369). A small river on the Swiss plateau unaffected by strong anthropic thermal alterations. The altitude of the catchment varies from 927 m a.s.l. to 445 m a.s.l, and the length of the main channel is about 26 km with a mean slope of 1.8%. The river flows through a sparsely inhabited area mainly devoted to agriculture. Temperature and discharge data are available for a period of 11 years (2002–2012). Further information in Iorgulescu et al. (2007).

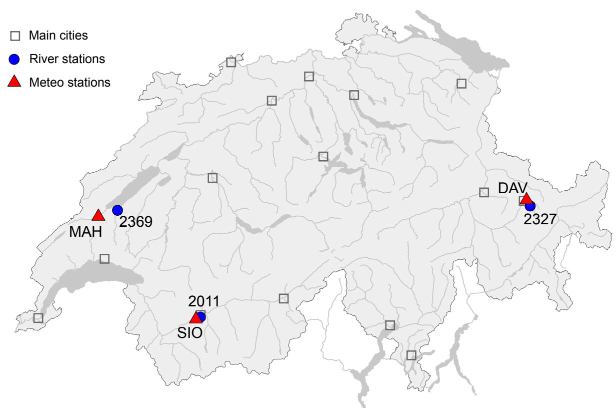

Figure 1: Map of Switzerland with the location of the stations considered in the analysis.

2. River Rhône at Sion (SIO-2011). A river affected by strong hydro- and thermo-peaking, and in general by the presence of cold waters that naturally leads to low summer water temperatures. The river lies at the bottom of a populated alpine valley, and its catchment is covered by glaciers for about 18%. Starting from the beginning of the 20^{th} century (with a rapid acceleration between the '50s and the '70s) its hydrological regime has been altered by the construction of a large high-head hydropower storage system (Hingray et al., 2010). A 30-year long record of temperature and discharge data is available, which covers the period 1984–2013.

3. River Dischmabach at Davos (DAV-2327). A river at high altitude with a significant influence of snow melting. The altitude of the catchment varies from 3146 m a.s.l. to 1668 m a.s.l., with a mean altitude of 2372 m a.s.l., and is covered by glaciers for about 2%. The main channel has a mean slope of 13% and flows for about 10 km through a glacial valley that is uninhabited and used for mountain pastures. Temperature and discharge measurements cover the 10-year period 2003–2012. Further information in Comola et al. (2015).

3 Net Heat Flux at the Air-Water Interface

The net heat flux per unit surface H [$\mathrm{W\,m^{-2}}$] at the air-water interface (defined as positive when directed towards the river) can be written as follows

$$H = H_s + H_a + H_w + H_l + H_c + H_p, \tag{1}$$

where H_s is the net short-wave radiative heat flux due to solar radiation actually absorbed by the water volume, H_a is the net long-wave radiation emitted from the atmosphere towards the river, H_w is the long-wave radiation emitted from the water, H_l is the latent heat flux due to evaporation/condensation, H_c is the sensible heat flux due to convection, and H_p is the heat flux due to incoming precipitation. In equation (1) we do not explicitly include water-sediments fluxes, as it is inherently accounted for in the formulation of the model by assuming that the volume of the river involved in the heat budget is in principle not limited to the water volume, but may include a portion of the saturated sediments.

The solar radiation approximately follows a sinusoidal annual cycle. Considering the short-wave reflectivity r_S (albedo) of the river surface, which is a function of the solar zenith angle, the net solar radiation H_s can be approximated as

$$H_s(t) = (1 - r_S) \left\{ s_0 + s_1 \cos\left[2\pi \left(\frac{t}{t_y} - s_2 \right) \right] \right\} , \tag{2}$$

where t is time, t_y is the duration of a year in the units of time considered in the analysis, and s_0, s_1, s_2 are coefficients that primarily depend on the latitude and the shading effects of local topography and vegetation. The effect of cloud cover is not explicitly considered in the present analysis.

Incoming and outgoing long-wave radiation is determined by the Stefan-Boltzmann equation, yielding to the following formulations

$$H_a(T_a, t) = (1 - r_a)\, \epsilon_a\, \sigma\, (T_K + T_a)^4 , \tag{3}$$

$$H_w(T_w) = -\epsilon_w\, \sigma\, (T_K + T_w)^4 , \tag{4}$$

where r_a is the reflectivity of the water for long-wave radiation, generally assumed to have a constant value (Henderson-Sellers, 1986), ϵ_a and ϵ_w are the emissivities of atmosphere and water, σ is the Stefan–Boltzmann constant ($5.67 \cdot 10^{-8}\,\mathrm{W\,m^{-2}\,K^{-4}}$), $T_K = 273.15\,\mathrm{K}$, and T_a and T_w are the temperatures of air and water expressed in Celsius [°C]. Water surface behaves almost like a black body, so the emissivity ϵ_w is essentially constant and close to unity. Differently, ϵ_a is more variable and depends on a number of factors including air temperature, humidity and cloud cover (Imboden and Wüest, 1995).

The sensible (H_c) and latent (H_l) heat fluxes can be calculated through the following bulk semi-empirical equations (Henderson-Sellers, 1986)

$$H_c(T_a, T_w, t) = \alpha_c\, (T_a - T_w) , \tag{5}$$

$$H_l(T_a, T_w, t) = \alpha_l\, (e_a - e_w) , \tag{6}$$

where α_c [$\mathrm{W\,m^{-2}\,K^{-1}}$] and α_l [$\mathrm{W\,m^{-2}\,hPa^{-1}}$] are transfer functions primarily depending on wind speed, stability of the lower atmosphere, and other thermophysical parameters, e_a is the vapor pressure of the atmosphere, and e_w is the water vapor saturation pressure at the temperature of water (both in [hPa]). The ratio α_c/α_e is known as Bowen coefficient and is generally taken constant ($\approx 0.61\,\mathrm{hPa\,K^{-1}}$) (Imboden and Wüest, 1995). The saturated water pressure e_w can be calculated through several empirical formulas essentially depending on temperature, as for example the following exponential law

$$e_w = a \exp\left(\frac{b\, T_w}{c + T_w} \right) , \tag{7}$$

where a=6.112 hPa, b=17.67 and c=243.5 °C (Bolton, 1980).

Assuming air and water temperature as the only independent variables of all flux components, equation (1) can be suitably linearised using Taylor series expansion around the long-term averaged values of these variables ($\overline{T}_a$ and $\overline{T}_w$, respectively), so that H can be rewritten as in equation (2) in the manuscript, where:

$$H|_{\overline{T}_a,\overline{T}_w} = H_s + H_a|_{\overline{T}_a} + H_w|_{\overline{T}_w} + H_l|_{\overline{T}_a,\overline{T}_w} + H_c|_{\overline{T}_a,\overline{T}_w} + H_p \,, \tag{8}$$

$$\left.\frac{\partial H}{\partial T_a}\right|_{\overline{T}_a,\overline{T}_w} = \left.\frac{\partial H_a}{\partial T_a}\right|_{\overline{T}_a} + \left.\frac{\partial H_l}{\partial T_a}\right|_{\overline{T}_a,\overline{T}_w} + \left.\frac{\partial H_c}{\partial T_a}\right|_{\overline{T}_a,\overline{T}_w} \,, \tag{9}$$

$$\left.\frac{\partial H}{\partial T_w}\right|_{\overline{T}_a,\overline{T}_w} = \left.\frac{\partial H_w}{\partial T_w}\right|_{\overline{T}_a} + \left.\frac{\partial H_l}{\partial T_w}\right|_{\overline{T}_a,\overline{T}_w} + \left.\frac{\partial H_c}{\partial T_w}\right|_{\overline{T}_a,\overline{T}_w} \,. \tag{10}$$

Then, we can rewrite equation (1) as

$$H = \rho\, c_p \left(\widehat{h}_0 + \widehat{h}_a T_a - \widehat{h}_w T_w\right) \,, \tag{11}$$

a form that is similar to equation (3) of the main text, but where the coefficients

$$\widehat{h}_0 = \frac{1}{\rho\, c_p} \left(H|_{\overline{T}_a,\overline{T}_w} - \left.\frac{\partial H}{\partial T_a}\right|_{\overline{T}_a,\overline{T}_w} \overline{T}_a - \left.\frac{\partial H}{\partial T_w}\right|_{\overline{T}_a,\overline{T}_w} \overline{T}_w \right) \,, \tag{12}$$

$$\widehat{h}_a = \frac{1}{\rho\, c_p} \left.\frac{\partial H}{\partial T_a}\right|_{\overline{T}_a,\overline{T}_w} \,, \qquad \widehat{h}_w = -\frac{1}{\rho\, c_p} \left.\frac{\partial H}{\partial T_w}\right|_{\overline{T}_a,\overline{T}_w} \,, \tag{13}$$

depend on time.

As a first approximation, we neglect the dependence of $\widehat{h}_a$ and $\widehat{h}_w$ on t, but retain it in $\widehat{h}_0$ by assuming a sinusoidal annual variation

$$\widehat{h}_0 = h_{00} + h_{01} \cos\left[2\pi \left(\frac{t}{t_y} - h_{02}\right)\right] \,, \tag{14}$$

analogously to the solar forcing (2). This kind of dependence was proven to be sufficient to reproduce the thermal dynamics in lakes (Piccolroaz et al., 2013).

However, since both T_a and T_w have an approximately sinusoidal behavior during the year, the net heat flux (11) is composed by three sinusoidal terms with the same periodicity, which give rise to a single term with amplitude and phase determined by the combination of the individual terms. In fact, given $A = a_0 + a_1 \cos(t - a_2)$ and $B = b_0 + b_1 \cos(t - b_2)$, it is straightforward to derive that $A + B = c_0 + c_1 \cos(t - c_2)$, with

$$\begin{aligned} c_0 &= a_0 + b_0 \,, \qquad c_1 = \sqrt{a_1^2 + b_1^2 + 2 a_1 b_1 \cos(a_2 - b_2)} \,, \\ c_2 &= \arctan\left[\frac{a_1 \sin(a_2) + b_1 \sin(b_2)}{a_1 \cos(a_2) + b_1 \cos(b_2)}\right] \,. \end{aligned} \tag{15}$$

As discussed in Piccolroaz et al. (2013), this potential over-parameterization can be avoided by removing the temporal dependence in (14) and relying on the proper combination of the parameters $\widehat{h}_a$ and $\widehat{h}_w$ multiplying T_a and T_w, respectively. The introduction of these assumptions leads to the formulation used in the model,

$$H = \rho\, c_p \left(h_0 + h_a T_a - h_w T_w\right) \,, \tag{16}$$

where the new parameters h_0, h_a and h_w are independent of time.

4 Analytical Solutions in Simple Cases

4.1 Sinusoidal Forcing

The model admits analytical solution in some idealized cases, as was also discussed by Toffolon et al. (2014). As a first approximation and only for the purposes to derive an explicit solution, we assume that the discharge (hence, θ and δ) is constant and that air temperature can be approximated by a sinusoidal forcing,

$$T_a = T_{a1} + T_{a2} \cos\left[2\pi\left(\frac{t}{t_y} - \varphi_a\right)\right] , \tag{17}$$

where T_{a1} is the annual average, T_{a2} the amplitude of its variation, and φ_a the phase of its maximum with respect to the first day of the year. Thus, we can rewrite the 8-parameter version as follows:

$$\delta\frac{dT_w}{dt} = A_1 + A_2 \cos\left[2\pi\left(\frac{t}{t_y} - \varphi_A\right)\right] - A_3 T_w , \tag{18}$$

where the right hand side represents the combined sinusoidal forcing term. The coefficients can be obtained by means of basic trigonometry:

$$\begin{aligned}
A_1 &= a_1 + a_2\, T_{a1} + a_5\, \theta , \\
A_2 &= \sqrt{(a_2 T_{a2})^2 + 2 a_2 T_{a2} a_6 \theta \cos\left[2\pi\left(\varphi_a - a_7\right)\right] + (a_6\theta)^2} , \\
\varphi_A &= \frac{1}{2\pi} \arctan\left[\frac{a_2 T_{a2} \sin\left(2\pi\varphi_a\right) + a_6\theta \sin\left(2\pi a_7\right)}{a_2 T_{a2} \cos\left(2\pi\varphi_a\right) + a_6\theta \cos\left(2\pi a_7\right)}\right] , \\
A_3 &= a_3 + a_8\, \theta .
\end{aligned} \tag{19}$$

We note that the coefficients of equation (18) for the other versions of the model can be easily derived by considering suitable values of the parameters, according to Table 1 in the manuscript. In particular, the 5-parameter version is obtained by imposing $\theta = 1$, $a_5 = 0$ and $a_8 = 0$, while the 4-parameter version with $a_5 = 0$, $a_6 = 0$ and $a_8 = 0$. The terms (19) for the 3- and 7-parameter versions are identical to the 4- and 8-parameter ones.

Equation (18) with constant coefficients admits a solution in closed form:

$$T_w = c_0 \exp\left(-\frac{t}{\tau}\right) + \widetilde{T}_w , \tag{20}$$

where $\tau = \delta/A_3$ is the time scale of the process. The first term on the right hand side of (20) describes the adaptation of the initial condition to the forcing (c_0 is a constant that can be calculated using the water temperature value at $t = 0$), while the second term represents the regime solution,

$$\widetilde{T}_w = T_{w1} + T_{w2} \cos\left[2\pi\left(\frac{t}{t_y} - \varphi_w\right)\right] , \tag{21}$$

where

$$T_{w1} = \frac{A_1}{A_3} ,$$

$$T_{w2} = \frac{A_2}{A_3\sqrt{1 + (2\pi\tau/t_y)^2}} \, ,$$
$$\varphi_w = \varphi_A + \frac{1}{2\pi} \arctan\left(\frac{2\pi\tau}{t_y}\right) \, . \tag{22}$$

It is immediate to recognize that A_3 is the main factor controlling the time scale of the process. If A_3 is large enough, τ becomes small (we can safely assume $\delta \sim O(1)$) so that the ratio $\tau/t_y \ll 1$. Under this assumption, the coefficients (22) can be cast in a simpler form as $T_{w2} \simeq A_2/A_3$ and $\varphi_w \simeq \varphi_A$. Interestingly, this latter case represents the so-called equilibrium solution T_{we} (e.g., Caissie et al., 2005), which is obtained by neglecting the temporal derivative in equation (18), thus leading to

$$T_{we} = \frac{A_1}{A_3} + \frac{A_2}{A_3} \cos\left[2\pi\left(\frac{t}{t_y} - \varphi_A\right)\right] \, . \tag{23}$$

4.2 Piecewise Forcing

We explicitly examine the situation where an abrupt change occurs in the forcing term. Focusing a short period in the analysis, we can rewrite the differential equation using constant coefficients

$$(\delta + \Delta\delta)\,\frac{dT_w}{dt} = A_0 + \Delta A - A_3 T_w \, , \tag{24}$$

where A_0 is the net heat flux at $t = 0$, ΔA is the change for $t > 0$, and $\Delta\delta$ a possible variation of the thermal inertia (e.g., due to variation of discharge and hence flow depth). As initial condition for $t = 0$, we assume the equilibrium temperature $T_{w0} = A_0/A_3$. The solution of this simple differential problem leads to

$$T_w = T_{w0} + \frac{\Delta A}{A_3}\left[1 - \exp\left(-\frac{A_3 t}{\delta + \Delta\delta}\right)\right] \, . \tag{25}$$

From this solution it is clear that we have to compare the adaptation time $\tau' = (\delta + \Delta\delta)/A_3$ with the time window we are using to describe the temporal variation of water temperature. For instance, if we are considering daily averaged T_w and τ' is shorter than one day, the delay in the adaptation to the external conditions can be neglected.

4.3 Instantaneous Adaptation

Keeping the same assumptions as in section 4.1 but considering a generic period of the oscillations of the overall forcing term, we can rewrite equation (18) in dimensionless form as

$$\epsilon \frac{dT_w^*}{dt^*} = b_1^* + b_2^* \cos(t^*) - T_w^* \, , \tag{26}$$

where $\epsilon = \omega\,\tau$, $T_w^* = T_w/\,\Delta T_w$, with ΔT_w a suitable scale for temperature difference, $t^* = \omega\, t - 2\pi\,\varphi_a$, with ω the generic angular frequency of the forcing (whereby we can consider annual variation, i.e. $\omega = 2\pi/t_y$, or much shorter fluctuations), $b_1 = A_1/(A_3\,\Delta T_w)$, and

$b_2 = A_2/(A_3\,\Delta T_w)$. If $\epsilon \ll 1$ (i.e., short τ), the solution can be obtained by means of a perturbation method. By introducing the expansion

$$T_w^* = T_{w0}^* + \epsilon\, T_{w1}^*\,, \tag{27}$$

the governing equation can be split into the base problem at $O(\epsilon^0)$,

$$T_{w0}^* = b_1^* + b_2^* \cos\left(t^*\right)\,, \tag{28}$$

which corresponds to the equilibrium solution (23), and the perturbed equation at $O(\epsilon)$,

$$T_{w1}^* = -\frac{dT_{w0}^*}{dt^*} = b_2^* \sin\left(t^*\right)\,. \tag{29}$$

We can now calculate the distance of solution (27), T_w^*, from its approximation obtained assuming instantaneous equilibrium, T_{w0}^*. The root mean squared difference between the two is given by

$$E^* = \sqrt{\overline{\left(T_w^* - T_{w0}^*\right)^2}} = \epsilon\sqrt{\overline{T_{w1}^*}^{\,2}} = \frac{\epsilon\, b_2}{\sqrt{2}}\,, \tag{30}$$

where the overbar denotes the average over the dimensionless period 2π of the fluctuations. Returning to dimensional variables and after some substitutions, it is possible to calculate the expected standard deviation of T_w with respect to the equilibrium solution,

$$E = E^*\,\Delta T_w = \frac{\delta}{\sqrt{2}}\frac{\omega\, A_2}{A_3^2}\,, \tag{31}$$

which shows that the equilibrium solution is acceptable if the ratio $(\omega\, A_2)/A_3^2$ is much smaller than E. This condition can be easily satisfied if we consider annual variations ($\omega \simeq 0.017$ day^{-1}). For variations occurring on a shorter time scale, a condition has to be posed on the parameter ratio to maintain E lower than a threshold E_0:

$$\frac{A_2}{A_3^2} < \frac{E_0\sqrt{2}}{\omega\,\delta}\,, \tag{32}$$

We can test the relationship (32) in the three examined cases, referring for simplicity to the 3-parameter version (for which $A_2 = a_2\, T_{a2}$ and $A_3 = a_3$). Considering, for instance, weekly fluctuations ($\omega \simeq 0.9$ day^{-1}), assuming $\delta \simeq 1$ and $T_{a2} \simeq 3$ K (corresponding to 6 K of variation of daily averaged water temperature during the week), and accepting errors $\sim$0.3 K, we obtain $A_2/A_3^2 < 0.5$ K day. The value of the ratio in the three cases is 3.6, 0.40, and 0.53, respectively, suggesting that the equilibrium solution can be adopted in case 2, and with a lower accuracy in case 3, while it will likely introduce relevant errors in case 1 (see Table 1 in the main text). Nonetheless, it should be noted that the estimate (31) does not account for the difference from the measured water temperature, which can be larger than the difference between the complete solution and its equilibrium approximation.

5 Particle Swarm Optimization Algorithm

The Particle Swarm Optimization (PSO) algorithm is an evolutionary and self-adaptive search optimization technique inspired by animal social behavior. The space of parameters is iteratively explored by a number N of particles. The position of the particles in the space of parameters identifies a set of parameters. The i-th particle moves within the parameters space by superimposition of 3 velocity components: a spatially constant drift $\mathbf{v}_i^k$, two random jumps whose amplitude depends on the distance of the particle from its best ($\mathbf{p}_{best,i}^k$, with p standing for partial) and from the global (community) best ($\mathbf{g}_{best}^k$, with g standing for global). Both bests are updated as the particles explore the domain finding better solutions. At each iteration k the position of the particles is updated according to the following expression:

$$\begin{aligned} \mathbf{v}_i^k &= w\,\mathbf{v}_i^{k-1} + c_1\,\mathbf{r}_1^k\,(\mathbf{p}_{best,i}^k - \mathbf{x}_i^k) + c_2\,\mathbf{r}_2^k\,(\mathbf{g}_{best}^k - \mathbf{x}_i^k)\,, \\ \mathbf{x}_i^k &= \mathbf{x}_i^{k-1} + \mathbf{v}_i^k\,, \end{aligned} \tag{33}$$

where w is an inertia weight, which reduces the drift with the number of iterations, c_1 and c_2 are constants known as cognitive and social learning factors, respectively, and $\mathbf{r}_1^t$ and $\mathbf{r}_2^t$ are uniformly distributed random numbers bounded between 0 and 1. Note that $\mathbf{x}$, $\mathbf{v}$, $\mathbf{p}$, $\mathbf{g}$, $\mathbf{r}_1$ and $\mathbf{r}_2$ are vectors with dimension equal to the number of parameters. Following the indications provided in the work of Robinson and Rahmat-Samii (2004), $c_1 = c_2 = 2$, and w has been set to vary linearly from $w_{ini} = 0.9$ at $t = 1$ to $w_{fin} = 0.4$ at $t = M$, where M is the total number of iterations. Finally, when a particle hits the boundary wall of the search space, the velocity component normal to the boundary is set to zero (absorbing wall boundary conditions).

6 Comparison among Models

Figure 2 illustrates the different performances of the various versions of the model (the corresponding values of the parameters are reported in Table 1).

As discussed in section 4.3 and in the main text, by neglecting the time derivative of the differential model the instantaneous equilibrium water temperature $T_{w,eq}$ can be derived:

$$T_{w,eq} = \frac{1}{(a_3 + \theta\,a_8)}\left\{a_1 + a_2 T_a + \theta\left[a_5 + a_6\,\cos\left(2\pi\left(\frac{t}{t_y} - a_7\right)\right)\right]\right\}\,. \tag{34}$$

The parameter a_4 is not present in equation (34), thus making the 8- and 4-parameter versions identical to the 7- and 3-parameter ones. Moreover, by rescaling the parameters by a_3 and defining the new parameters e_i (i from 1 to 6, see the main text), the total number of degrees of freedom of the equilibrium temperature is reduced of one unit with respect to the differential versions of the model. Figure 4 shows the performances of the three equilibrium relationships defined in the main text, and Table 2 reports the values of the parameters. Moreover, Figure 3 shows the difference between the 8-parameter version of the model and its equilibrium version.

Table 1: Values of the Calibrated Parameters.

	a_1 [^{o}C d^{-1}]	a_2 [d^{-1}]	a_3 [d^{-1}]	a_4 [-]	a_5 [^{o}C d^{-1}]	a_6 [^{o}C d^{-1}]	a_7 [-]	a_8 [d^{-1}]
Case 1 (natural)								
8-par	0.889	0.649	0.765	0.129	2.318	1.536	0.603	0.241
7-par	0.912	0.623	0.741	-	1.764	1.189	0.607	0.182
5-par	3.149	0.708	1.059	-	-	1.632	0.585	-
4-par	0.935	0.504	0.620	0.212	-	-	-	-
3-par	1.002	0.549	0.674	-	-	-	-	-
Case 2 (regulated)								
8-par	0.346	0.219	0.178	0.718	7.773	2.217	0.529	1.280
7-par	1.165	0.192	0.292	-	3.631	1.224	0.520	0.665
5-par	9.172	0.351	1.834	-	-	1.303	0.485	-
4-par	9.303	0.531	2.110	-0.251	-	-	-	-
3-par	8.072	0.455	1.827	-	-	-	-	-
Case 3 (snow-fed)								
8-par	4.794	0.629	1.410	0.270	0.000	4.912	0.582	0.637
7-par	3.536	0.455	1.073	-	0.000	3.080	0.587	0.384
5-par	7.486	0.651	2.768	-	-	7.044	0.607	-
4-par	5.917	0.929	2.285	-0.147	-	-	-	-
3-par	5.803	0.923	2.277	-	-	-	-	-

Table 2: Values of the Parameters for Equilibrium Water Temperature Relationships.

	e_1 [^{o}C]	e_2 [-]	e_3 [-]	e_4 [-]	e_5 [^{o}C]	e_6 [^{o}C]
Case 1 (natural)						
6-par	1.20	0.84	0.60	0.44	4.30	2.96
4-par	3.50	0.62	0.58	-	-	2.02
2-par	1.64	0.80	-	-	-	-
Case 2 (regulated)						
6-par	2.70	0.90	0.53	4.64	28.20	7.95
4-par	5.04	0.19	0.49	-	-	0.74
2-par	4.43	0.25	-	-	-	-
Case 3 (snow-fed)						
6-par	3.61	0.44	0.58	0.44	-0.36	3.68
4-par	3.25	0.25	0.59	-	-	-1.64
2-par	2.60	0.40	-	-	-	-

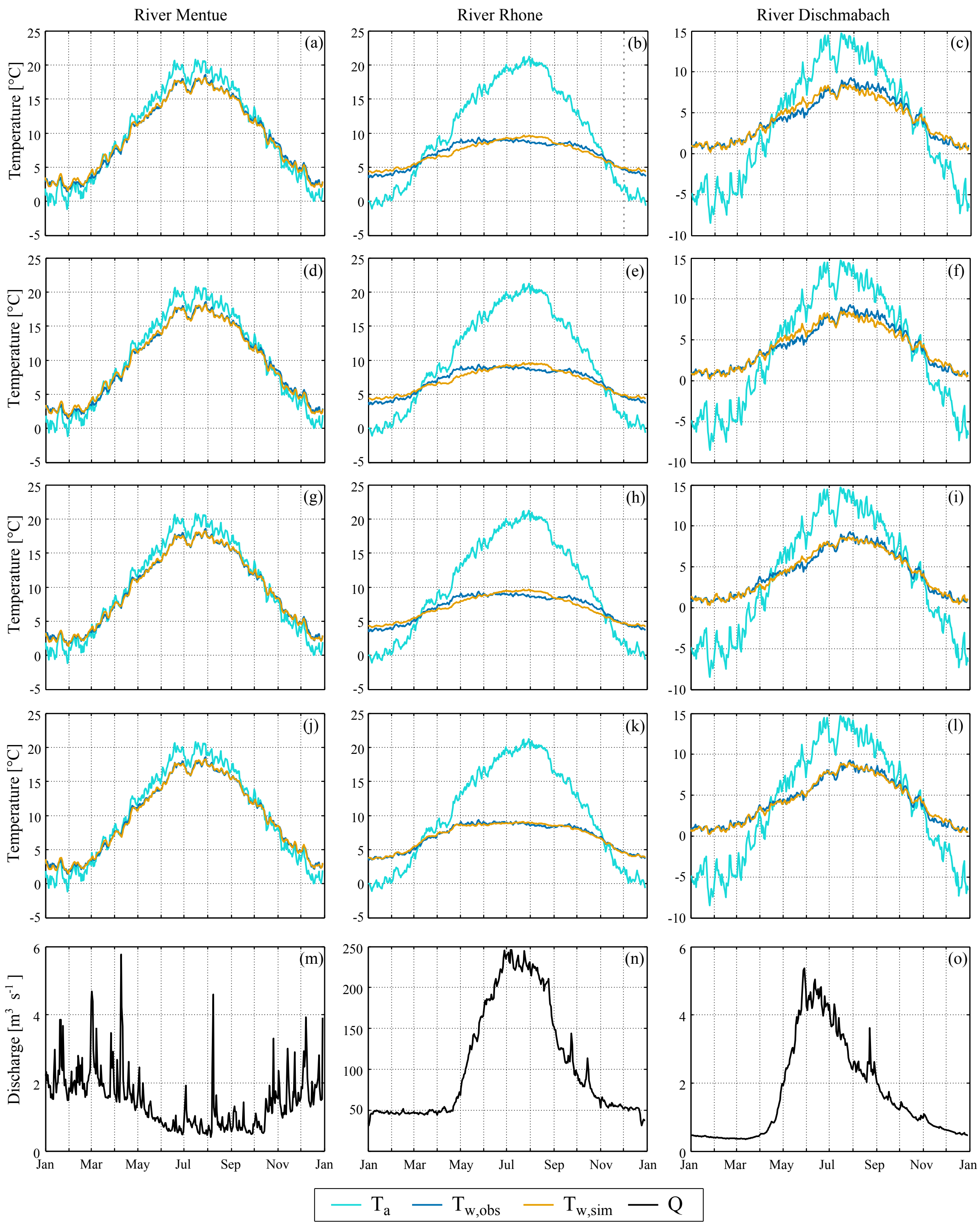

Figure 2: Mean year of the variables for the three case studies (columns): (a-l) measured air temperature (T_a), observed ($T_{w,obs}$) and simulated ($T_{w,sim}$) water temperature; (m-o) measured discharge (Q). The different versions of the model are (from top to bottom): (a-c) 3-parameter, (d-f) 4-parameter, (g-i) 5-parameter, (j-l) 7-parameter.

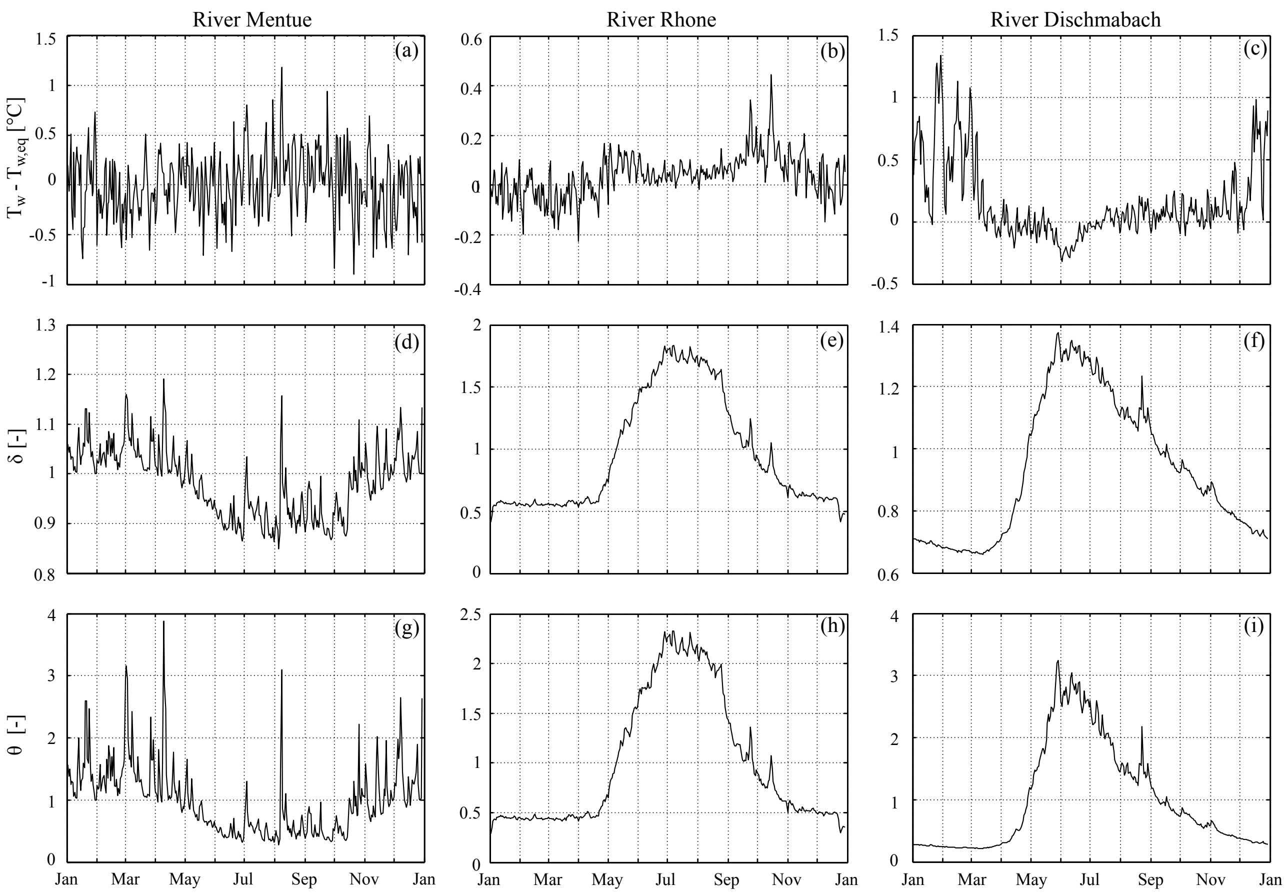

Figure 3: Difference between the solution T_w of differential equation (7) of the main text (8-parameter model) and its approximation $T_{w,eq}$ obtained by assuming instantaneous adaptation (equation (10) of the main text), for the three case studies (columns): (a-c) $T_w - T_{w,eq}$; (d-f) dimensionless volume ratio δ; (g-i) dimensionless discharge θ.

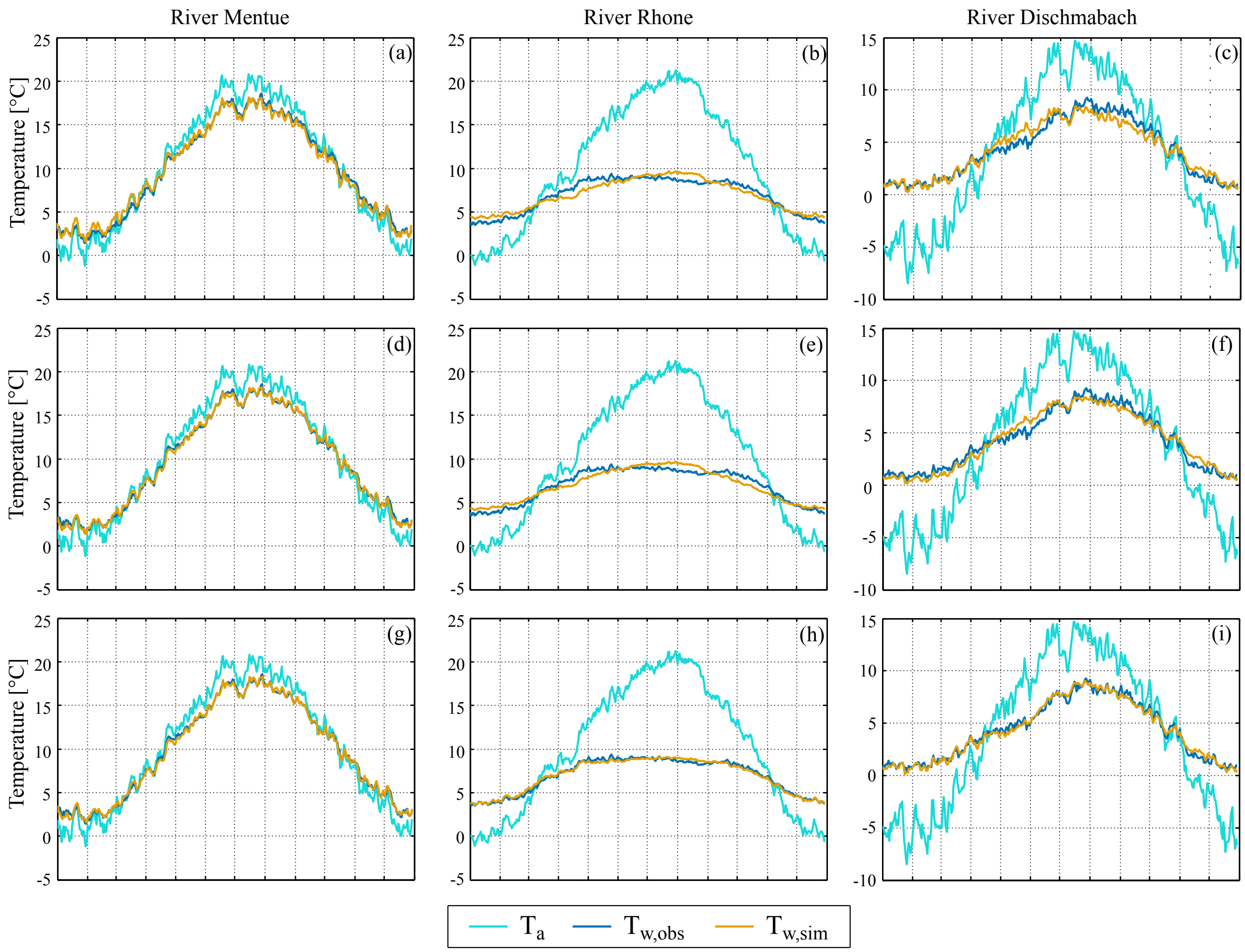

Figure 4: Water temperature ($T_{w,sim}$) simulated assuming equilibrium conditions (i.e., $T_{w,eq}$), together with observed water temperature ($T_{w,obs}$) and air temperature (T_a): (a-c) 2-parameter $T_{w,eq}$; (d-f) 4-parameter $T_{w,eq}$; (g-i) 6-parameter $T_{w,eq}$. The discharge used for the three cases in subplots (g-i) is the same as in Figure 2(m-o).

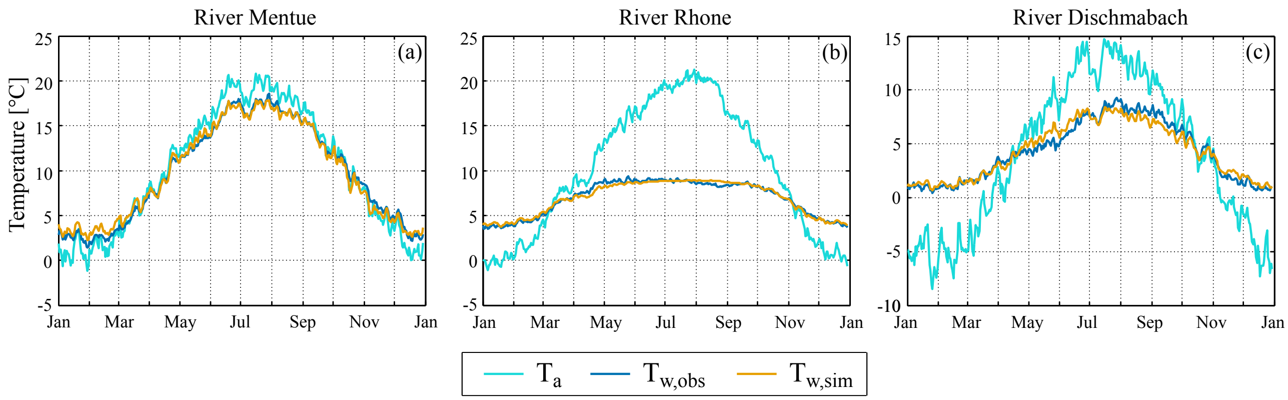

Figure 5: Water temperature ($T_{w,sim}$) simulated using the logistic regression, equation (35), together with observed water temperature ($T_{w,obs}$) and air temperature (T_a).

Table 3: Values of the Parameters for Logistic Regression.

Case	μ	α	β	γ
	[°C]	[°C]	[°C]	[°C^{-1}]
1 (natural)	0.00	21.2	11.3	0.183
2 (regulated)	2.67	9.00	5.36	0.280
3 (snow-fed)	0.00	10.4	6.62	0.189

The *air2stream* model has also been compared against the most common nonlinear regression model based on the logistic function (Mohseni et al., 1998)

$$T_w = \mu + \frac{\alpha - \mu}{1 + \exp\left[\gamma\left(\beta - \widehat{T}_a\right)\right]}\,, \tag{35}$$

which correlates water temperature to air temperature. When calculating T_w at day i, $\widehat{T}_a$ in equation (35) has been estimated as the mean between the daily averaged air temperatures at day i and $i-1$. This has been proven to provide better results with respect to using T_a either at day i or at day $i-1$. The performance of the regression model (35) are shown in Figure 5, and the value of the parameters are reported in Table 3.

It is worth noting that the 4-parameter equilibrium relationship, derived from the 5-parameter version of the differential model, has the same degree of freedom as the logistic regression. This allows for a direct comparison in terms of performances. Moreover, the 2-parameter equilibrium relationship, derived from the 4-parameter version of the differential model, corresponds to a linear regression, with the only difference that the model is characterized by a lower bound at 0°C.

References

Bolton, D. (1980), The Computation of Equivalent Potential Temperature, *Mon. Wea. Rev.*, *108*, 1046–1053, doi:10.1175/1520-0493(1980)108<1046:TCOEPT>2.0.CO%3B2.

Caissie, D., M. G. Satish, and N. El-Jabi (2005), Predicting river water temperatures using the equilibrium temperature concept with application on Miramichi River catchments (New Brunswick, Canada), *Hydrol. Processes., 19*(11), 2138–2159, doi:10.1002/hyp.5684.

Comola, F., B. Schaefli, A. Rinaldo, and M. Lehning (2015), Thermodynamics in the hydrologic response: Travel time formulation and application to Alpine catchments, *Water Resour. Res.*, doi:10.1002/2014wr016228.

Henderson-Sellers, B. (1986), Calculating the surface energy balance for lake and reservoir modeling: A review, *Rev. Geophys., 24*(3), 625–649, doi:10.1029/RG024i003p0062.

Hingray, B., B. Schaefli, A. Mezghani, and Y. Hamdi (2010), Signature-based model calibration for hydrologic prediction in mesoscale Alpine catchments, *Hydrological Sciences Journal, 55*, 1002–1016, doi:10.1080/02626667.2010.505572.

Imboden, D. M., and Wüest, A. (1995), 4 Mixing Mechanisms in Lakes, in Physics and Chemistry of Lakes, pp. 83–138, Springer Berlin Heidelberg.

Iorgulescu, I., K. J. Beven, and A. Musy (2007), Flow, mixing, and displacement in using a data-based hydrochemical model to predict conservative tracer data, *Water Resour. Res., 43*, W03401, doi:10.1029/2005wr004019.

Mohseni O., H. G. Stefan, and T. R. Erickson (1998), A nonlinear regression model for weekly stream temperatures, *Water Resour. Res., 34*, 2685–92.

Piccolroaz, S., M. Toffolon, and B. Majone (2013), A simple lumped model to convert air temperature into surface water temperature in lakes, *Hydrol. Earth Syst. Sci., 17*, 3323-3338, doi:10.5194/hess-17-3323-2013.

Robinson, J., and Y. Rahmat-Samii (2004), Particle swarm optimization in electromagnetics, *IEEE T. Antenn. Propag., 52*, 397-407, doi:10.1109/TAP.2004.823969.

Toffolon, M., S. Piccolroaz, B. Majone, A.-M. Soja, F. Peeters, M. Schmid, and A. West (2014), Prediction of surface temperature in lakes with different morphology using air temperature, *Limnol. Oceanogr., 59*(6), 2182-2202, doi:10.4319/lo.2014.59.6.2185.